2001

Kinetics and Mechanism of Birnessite Reduction by Catechol

Christopher J. Matocha
University of Kentucky, cjmato2@pop.uky.edu

Donald L. Sparks
University of Delaware

James E. Amonette
Pacific Northwest National Laboratory

Ravi K. Kukkadapu
Pacific Northwest National Laboratory, ravi.kukkadapu@pnl.gov

DIVISION S-2—SOIL CHEMISTRY

Kinetics and Mechanism of Birnessite Reduction by Catechol

Christopher J. Matocha,* Donald L. Sparks, James E. Amonette, and Ravi K. Kukkadapu

ABSTRACT

The complex interactions of oxidizable organic ligands with soil Mn(III,IV) (hydr)oxide minerals have received little study by in situ spectroscopic techniques. We used a combination of an in situ electron paramagnetic resonance stopped-flow (EPR-SF) spectroscopic technique and stirred-batch studies to measure the reductive dissolution kinetics of birnessite (δ-MnO_2), a common Mn mineral in soils, by catechol (1,2-dihydroxybenzene). The reaction was rapid, independent of pH, and essentially complete within seconds under conditions of excess catechol at pH 4 to 6. The overall empirical second-order rate equation describing the reductive dissolution rate was $d[Mn(II)]/dt = k[CAT]^{1.0}[SA]^{1.0}$ where $k = 4$ (± 0.5) (10^{-3} L m^{-2} s^{-1} and [CAT] and [SA] are the initial concentrations in molarity and meters square per liter. In the process, catechol was oxidized to the two-electron *o*-quinone product. The energy of activation (E_a) for the reaction was 59 (± 7) kJ mol^{-1} and the activation entropy ($S^{\ddagger}$) was -78 ± 22 J mol^{-1} K^{-1}, suggesting that the reaction was surface-chemical controlled and occurs by an associative mechanism. Rates of catechol disappearance from solution with simultaneous Mn(II) and *o*-quinone production were comparable. These data strongly suggest that precursor surface-complex formation is rate-limiting and that electron transfer is rapid. The rapid reductive dissolution of birnessite by catechol has significant implications for C and Mn cycling in soils and the availability of Mn to plants.

Behavior of Mn in soils and geochemical sediments is generally assumed to be mediated by redox reactions. Data based on frontier molecular orbital theory (FMOT) considerations (Luther, 1990) show that oxides and hydroxides containing Mn(III) and Mn(IV) can oxidize organic ligands more rapidly than O_2. Aromatic and nonaromatic ligands have been reported to dissolve reductively Mn(III,IV) (hydr)oxides (Stone and Morgan, 1984a,b) with the formation of polymeric reaction products that resemble soil humic substances (Shindo and Huang, 1982, 1984). Sorbed contaminants can be released into solution following reductive dissolution of solid Mn(III,IV) (hydr)oxides by organic ligands and reactive compounds may be sorbed or coprecipitated as a consequence of hydrolysis of the Mn(II) that is released (Xyla et al., 1992; Godtfredsen and Stone, 1994; Larsen and Postma, 1997). Thus, redox cycling of Mn is dynamic and coupled to geochemical cycling of other metals, C turnover in soils, and N transformations in soils and marine sediments (Hem, 1978; Bartlett, 1981; Wang and Huang, 1987, 1992; Laha and Luthy, 1990; Luther et al., 1997; Naidja et al., 1998).

Pivotal early investigations into oxidizable organic ligand reactions with solid Mn(III,IV) (hydr)oxides postulated that the formation of a precursor surface complex is requisite to electron transfer and that inner-sphere electron transfer or reactions involving surface species were rate-limiting (Stone and Morgan, 1984a,b; Xyla et al., 1992). No direct measurements of reductant sorption can be made in most reductive dissolution studies because of the rapid reduction of Mn(III,IV) (hydr)oxides; however, dissolution rates are directly proportional to the concentration of the surface complex (Xyla et al., 1992). The only direct line of evidence in support of an inner-sphere mechanism was the study conducted by Gordon and Taube (1962) using ^{18}O-labeled water. These authors found that the UO_2^{2+} produced by the reaction of MnO_2 with U(IV), derived both oxygen atoms from MnO_2.

A previous EPR spectroscopic measurements showed

C.J. Matocha, Dep. of Agronomy, Univ. of Kentucky, N-122 Ag. Sci. Ctr-North, Lexington, KY 40546-0091; D.L. Sparks, Dep. of Plant and Soil Sciences, 147 Townsend Hall, Univ. of Delaware, Newark, DE 19717-1303; J.E. Amonette and R.K. Kukkadapu, William R.Wiley Environmental Molecular Sciences Lab. (EMSL), Pacific Northwest National Lab., Richland, WA 99352. Received 20 Aug. 1999. *Corresponding author (cjmato2@pop.uky.edu).

Published in Soil Sci. Soc. Am. J. 65:58–66 (2001).

that soluble Mn(II) release from birnessite after reaction with catechol was rapid (McBride, 1989a,b). Catechol dissolved MnO_2 more rapidly than hydroquinone because it is a bidentate ligand able to chelate surface Mn metal centers (Stone and Morgan, 1984a,b; McBride, 1989a,b). However, few rate coefficients describing Mn(II) release were measured in these systems. The disequilibrium in aqueous redox reactions commonly observed in the field (Lindberg and Runnels, 1984) underscores the need for kinetic studies (Sparks, 1989; Bartlett and James, 1993; Stone et al., 1994).

Recent investigations have demonstrated that dynamic redox reactivity of Mn(III,IV) (hydr)oxide mineral surfaces catalyzes abiotic degradation of organic pollutants (Ukrainczyk and McBride, 1993a,b; Dec and Bollag, 1994; Pizzigallo et al., 1995; Cheney et al., 1996). In fact, oxidation of catechol to CO_2 by birnessite has been reported and could contribute to significant abiotic degradation of organic contaminants in natural settings (Wang and Huang, 1992; Naidja et al., 1998). This finding is surprising because degradation of organic pollutants has generally been attributed to biological activity.

From this discussion, it is evident that oxidizable organic ligand interactions with Mn(III,IV) (hydr)oxide minerals in soils are complex. Soil Mn oxides are the principal source of plant available Mn(II) and, thus, pathways of reduction influence plant toxicity and disease resistance (Schulze et al., 1995a). Better understanding of the chemistry of these interactions improves our ability to make sound predictions about contaminant fate, cleanup, and plant available Mn(II). Most of the available reductive dissolution kinetics data have been macroscopic measurements (Stone et al., 1994) with few in situ spectroscopic studies.

To understand adequately the complex reactivity of Mn(III,IV) (hydr)oxides with organic ligand reductants in soils, however, it is best to begin with simpler model systems and combine in situ molecular-level spectroscopic techniques with macroscopic investigations to provide mechanistic kinetic information (Sparks, 1995). In this regard, catechol is a suitable model organic ligand because ortho-type semiquinones have been identified in soil humic substances (Steelink, 1964), catechols are common intermediates in pesticide degradation pathways (Alexander, 1977), and they have been identified on siderophore molecules (Hersman et al., 1995). Birnessite is a suitable model mineral because it is one of the most commonly identified Mn oxide minerals in soils and geochemical environments (McKenzie, 1989). Our approach to the problem, then, involved a study of the kinetics and mechanism of reductive dissolution of well-characterized birnessite by catechol using in situ EPR-SF and stirred-batch techniques.

MATERIALS AND METHODS

Birnessite Preparation and Characterization

Birnessite was synthesized according to procedures outlined by McKenzie (1971) by reduction of boiling $KMnO_4$ with concentrated HCl. The precipitate was vacuum filtered, dialyzed against deionized water to remove salts, and freeze-dried. Total concentrations of Mn and K were determined by dissolving a known solid weight with 12 *M* HCl and acidified $NH_2OH{\cdot}HCl$. Powder X-ray diffraction (XRD) analysis revealed that diagnostic d-spacings for birnessite agreed with published values (Table 1). Point of zero charge (PZC) was estimated for birnessite by microelectrophoretic mobility measurements as a function of pH in 1 m*M* NaCl and 3.2 $m^2\ L^{-1}$ surface area concentration (Murray, 1974). Increased negative electrophoretic mobilities were observed for unreacted birnessite as pH increased and extrapolation to zero revealed a PZC of 1.81 ± 0.04 (Table 1). These results are consistent with those reported in the literature for birnessite (Balistrieri and Murray, 1982; Murray, 1974). Oxidation state was measured iodometrically by a starch end point and standardized thiosulfate solution (Murray et al., 1984; Amonette et al., 1994). Pyrophosphate ($P_2O_7^{4-}$)-extractable Mn(III) was measured by reacting large excesses of $P_2O_7^{4-}$ (50 m*M*) with birnessite (~2.7 mM Mn_T) at pH 4 and 23°C or 33°C by published procedures (Diebler and Sutin, 1964; Davies, 1969; Kostka et al., 1995). High resolution thermogravimetric analysis (HRTGA, TA Instruments) was used to measure both structural and adsorbed H_2O contents. High-resolution ramp mode at a heating rate of 10°C min^{-1} under flowing N_2 was used with Pt crucibles to measure total H_2O content, which is operationally defined as the weight loss after heating to 300°C (Moore et al., 1990).

Table 1. Selected physical and chemical properties of birnessite.

Property	Birnessite
Total Mn, %	49.1 ± 0.1†
Total K, %	16.0 ± 0.1
Total H_2O, %	12.4
Mean Oxidation State	3.4 ± 0.1
BET Surface Area, $m^2\ g^{-1}$	40.0
PZC	1.81 ± 0.04
$P_2O_7^{4-}$ Mn(III), %	10.0
XRD, nm	0.732, 0.362, 0.246, 0.142

† Standard error of the mean.

Birnessite was further characterized by x-ray absorption spectra recorded at beamline X-11A at the National Synchrotron Light Source, Brookhaven National Laboratory, Upton, NY. Beam energy was calibrated to the K-absorption edge of Mn metal foil (6539 eV). The spectra were collected in fluorescence mode with a Lytle detector and compared with a standard Mn(IV) dioxide phase pyrolusite (β-MnO_2). Corundum (α-Al_2O_3) was used as a diluent to minimize self-absorption effects (Schulze et al., 1995b). Comparison of pre-edge XANES spectra of birnessite to reference pyrolusite (iodometric oxidation state of 3.92) showed agreement with published pre-edge energies reported by Manceau et al. (1992). Recent structural refinements of this mineral phase have shown that structural Mn(III) is present in birnessite, often substituted for Mn(IV) in the lattice (Drits et al., 1997; Silvester et al., 1997). External surface area was measured by the BET procedure using N_2 (g) as the adsorbate (Brunauer et al., 1938).

Stirred-Batch Experiments

Stirred-batch reductive dissolution rate experiments were conducted by a pH-stat (±0.1 pH units) technique while purging with purified N_2 at 10, 15, 18, and 23°C. Temperature was controlled with a circulating water bath. Birnessite mineral suspensions were dispersed by sonification and pretreated at the experimental pH value and ionic strength prior to catechol addition. Reactions were initiated by addition of a weighed aliquot of catechol stock solution buffered to the desired pH with dilute 0.1 *M* NaOH or 0.1 *M* HCl. Catechol stock solutions

were freshly prepared prior to each experimental run. Sample aliquots were removed at increasing time intervals and passed through a 0.2-μm pore-size membrane filter into a tared plastic tube and acid-quenched. Soluble Mn in the filtrates was measured with flame atomic absorption spectrometry (AAS). The UV-VIS spectra of the filtrates in 1-cm cuvettes were recorded to follow formation of products during the reaction sequence with an HP 8452A Diode Array UV-VIS spectrophotometer. Literature values for the *o*-quinone monomer were taken from Mentasti et al. (1975) as 1460 M^{-1} cm^{-1} at 390 nm. For catechol, Beer's law was obeyed at concentrations ≤0.5 m*M* catechol at 276 nm and yielded ε = 2380 M^{-1} cm^{-1}. At longer times (>2 min), competing reactions involving the unstable *o*-quinone monomer with water and unreacted catechol are operative (Dawson and Nelson, 1938; Mason, 1949). Corrections were made for removal of suspension volume from the batch reactor during sampling in calculating acid consumption. Mn(II) that was added concurrently with catechol at the beginning of the kinetic run had a negligible influence on the overall reductive dissolution rate. No significant differences were observed between the presence and absence of a N_2 purge.

EPR-SF Kinetic Studies

Reductive dissolution of birnessite by catechol was followed in situ by an EPR-SF technique (Klimes et al., 1980; Stach et al., 1985; Fendorf et al., 1993) to measure Mn(II) release and detect possible semiquinone intermediates. The six-line diagnostic EPR spectra confirmed that birnessite was reduced to Mn(II) during the reaction with catechol (Fig. 1a). The hyperfine spectrum of high spin Mn(II) is due to coupling of the electron spin (S = 5/2) to the nuclear spin (I = 5/2) of the ^{55}Mn ion.

Spectra were recorded at room temperature (23° ± 0.5°C) and a microwave frequency of 9.55 GHz (X-band) with a Bruker ESP 300E spectrometer. Mixed samples were injected by the stopped-flow (SF) unit (Update Instruments, Inc., Madison, WI) into a flow-through quartz flat aqueous cell (Wilmad Glass Co., Buena, NJ) inserted in a TE_{102} resonator. A microwave power attenuation of 30 dB and modulation amplitude of 10^{-3} T were employed and this power rating was checked to ensure that no saturation effects occurred for the highest Mn(II) concentration (Luca and Cardile, 1989). When the entire six-line spectrum for Mn(II) was desired, field-sweep mode was used (0.05 T). Data processing was done with BRUKER software (WINEPR).

Stopped-flow kinetic measurements were made with ms time resolution in time-sweep mode by centering on the *increase* in intensity of the fourth downfield resonance peak (H_o in Fig. 1a) at 0.3435 T (g = 1.98) during the reaction sequence. This peak is the most suitable one for quantitative measurements of Mn(II) (Carpenter, 1983). This approach has been used by others in EPR-SF studies (Fendorf et al., 1993). A parallel experiment centering on the "valley" at 0.346 T (H_1 in Fig. 1a) showed a decrease in intensity with time which confirmed that H_0 intensities corresponded to release of Mn(II) following reductive dissolution of birnessite. Signal intensities were converted to concentration using $MnCl_2$ standards prepared in the same suspension matrix as the samples. The same $MnCl_2$ standards were analyzed with flame AAS to intercorrelate the methods. The EPR technique yielded a linear response to Mn(II) between 5 and 200 μ*M* (Fig. 1b).

The SF system consisted of a syringe ram (model 1019), ram controller (model 715), 2-mL syringes, and a Wiskindgrid mixing cell. The mixing cell had a dead volume of 1.6 L. Details of this system can be found elsewhere (Hubbell et al., 1987). The mixing cell was attached by tubing to the quartz flat aqueous cell located in the EPR cavity. Before starting the reaction, the magnetic field was swept to ensure no residual Mn(II) remained in the flat cell between experimental runs.

Kinetic studies were conducted under pseudo-first-order conditions with either catechol or birnessite in excess. Catechol concentrations ranged from 200 to 10 000 μ*M* and birnessite suspension surface area concentrations ranged from 0.45 to 4.5 m^2 L^{-1}. Total Mn concentrations as birnessite (100–500 μ*M*) when in deficit (catechol in excess) reflect typical environmental concentrations of Mn. Experiments were conducted at initial pH values of 4, 4.5, 5, and 6 as maintained by a 50 m*M* K-acetate buffer. Additional experiments indicated that K-acetate buffer did not significantly influence Mn(II) release rates when compared with the pH-stat method. Adjustments of the buffer to the desired pH were made with aliquots of concentrated HCl and pH was measured with a model 25 pH/ion meter (Fisher Scientific Co., Pittsburgh, PA). Small drifts in pH values (±0.05) during the reactions were due to the finite capacity of the K-acetate buffer. The low ionic strength coupled with the dilute solids concentration was sufficient to keep birnessite dispersed during the time period of the experimental runs. In addition, birnessite suspensions

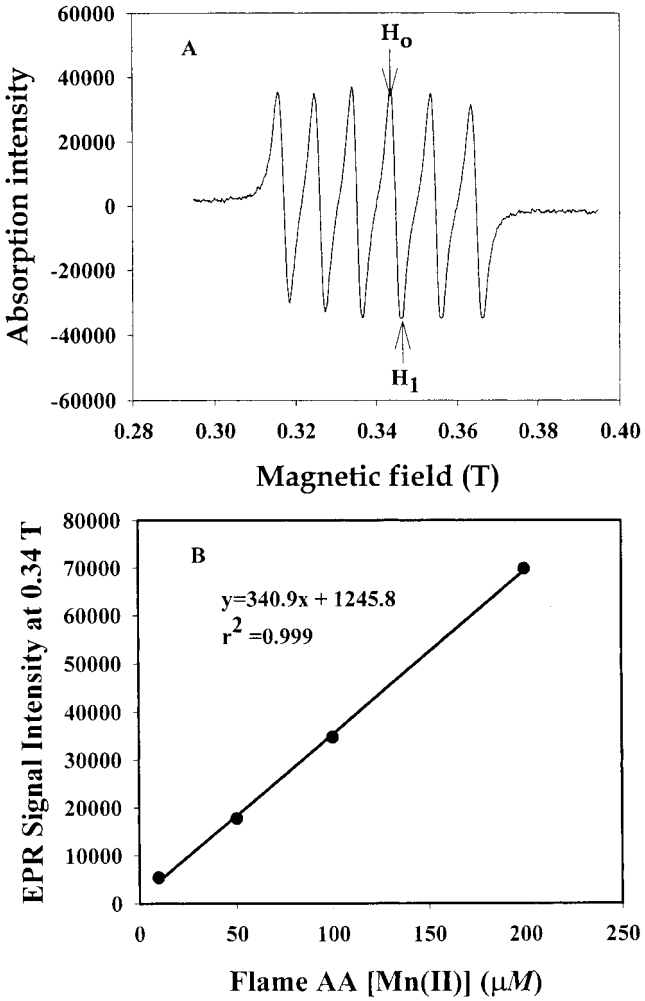

Fig. 1. (A) Representative room temperature EPR spectra of 100 μ*M* Mn_T as birnessite (0.45 m^2 L^{-1}) reacted with catechol (5 × 10^{-3} *M*) depicting the characteristic six-line spectra of the Mn(II) product. H_0 and H_1 indicate the peak and valley used to quantify Mn(II) concentrations. (B) Intercalibration standard curve relating EPR signal intensity at the 0.3435 T (H_0) peak to flame AAS Mn(II) concentration.

were sonified prior to filling the inport syringes. Sweep times were set to either 20 or 83s, depending on the experimental conditions, with a temporal resolution of 4096 time steps. The data collection software was configured to automatically trigger a series of field-sweeps of the reacted suspensions immediately after time-sweep mode kinetic measurements to ensure that there were no shifts in the resonance peak and to assist in quantifying final Mn(II) concentrations. The method of initial rates (Lasaga, 1981) was used to ensure that the forward reaction predominated and competing reactions with catechol oxidation products were not operative (Stone, 1987; Sparks, 1995).

RESULTS AND DISCUSSION

EPR-SF and Stirred-Batch Kinetic Studies

Reductive dissolution of birnessite ($E° = 1.29$ V, Bricker, 1965) by catechol is favored thermodynamically between pH 4 ($\Delta G_r = -92$ kJ mol^{-1}) and pH 6 ($\Delta G_r = -69$ kJ mol^{-1}) for [Mn^{2+}], [CAT], and [*o*-quinone] of 1, 1000, and 1 μM. On the basis of the predicted stoichiometry, slightly more protons were consumed per mole Mn(II) released (Fig. 2):

$$\delta\text{-}MnO_{1.7}(s) + 0.7C_6H_4(OH)_2 + 2H^+ \rightarrow Mn(II)(aq) + 0.7C_6H_4O_2(aq) + 1.7H_2O \quad [1]$$

and the appearance of the two-electron *o*-quinone product (see discussion below). Representative EPR-SF kinetics of the reductive dissolution of birnessite by catechol revealed that the reaction was rapid and essentially complete in <10 s when catechol is in excess (Fig. 3). On the basis of a previous study with feitknechtite (Stone and Morgan, 1984a), the rate of Mn(II) production as a function of birnessite concentration, catechol concentration, and pH, can be described by

$$d[Mn(II)]/dt = k_{obs}[CAT]^a[SA]^b[H^+]^c \quad [2]$$

where $d[Mn(II)]/dt$ is the rate of Mn(II) production (M s^{-1}), [CAT] is the initial concentration of catechol (M), [SA] is the surface area concentration of the birnessite suspension (m^2 L^{-1}), [H^+] is the hydrogen ion concentration (M), k_{obs} is the apparent rate constant, and a, b, and c are the reaction orders with respect to the given reactants. The initial rate approach (Lasaga, 1981) was employed to determine the empirical rate equation. The value for $d[Mn(II)]/dt$ was taken from the initial linear slopes when <20% of the reaction had occurred.

An initial rate plot of log [Mn(II)] release versus log [CAT] was linear ($r^2 = 0.95$) with a slope (a) of 1.06, indicating a first order dependence of the reaction rate on [CAT] at pH 4 (Fig. 4a). The pseudo-first-order rate coefficient, k', was shown from the y-intercept to be 5×10^{-3} s^{-1}. By considering the nonvaried reactant, the rate constant k_{graph} was calculated by the following relationship

$$k' = k_{graph}[SA]^b \quad [3]$$

resulting in a value of 5.55×10^{-3} L m^{-2} s^{-1}. This value agreed with the average k_{calc} determined from the empirical second-order equation and relevant data in Table 2 (average $k_{calc} = 4 \times 10^{-3}$ L m^{-2} s^{-1} for [CAT] of 10^{-3}-10^{-2} M, [SA] = 0.9 m^2 L^{-1}, [H^+] = 10^{-4} M). Similiarly, the initial rate plot for [SA] was linear ($r^2 = 0.95$) with a first-order dependence on [SA] (Fig. 4b). The k_{graph} value obtained from the y-intercept of 2.6×10^{-3} L m^{-2} s^{-1} was in good agreement with the average k_{calc} of 2.6×10^{-3} L m^{-2} s^{-1} (Table 2). The initial rate of Mn(II) release from birnessite was virtually independent of pH with a slope near 0 in the pH range 4 to 6 (Fig. 4c). Apparently, the [H^+] term did not directly participate in the rate equation (see Eq. [2]) despite the observed consumption of H^+ in Eq. [1]. In their studies with feitknechtite, Stone and Morgan (1984a) reported a first-order dependence on both hydroquinone and suspension loading, but a reaction order of 0.46 for [H^+]. The overall empirical second-order rate equation describing the reductive dissolution of birnessite by catechol can be written as

$$d[Mn(II)]/dt = k[CAT]^{1.0}[SA]^{1.0} \quad [4]$$

where $k = 4 (\pm 0.5) \times 10^{-3}$ L m^{-2} s^{-1} and [CAT] and [SA] are the initial concentrations in M and m^2 L^{-1}. The reasonable agreement between the apparent second-

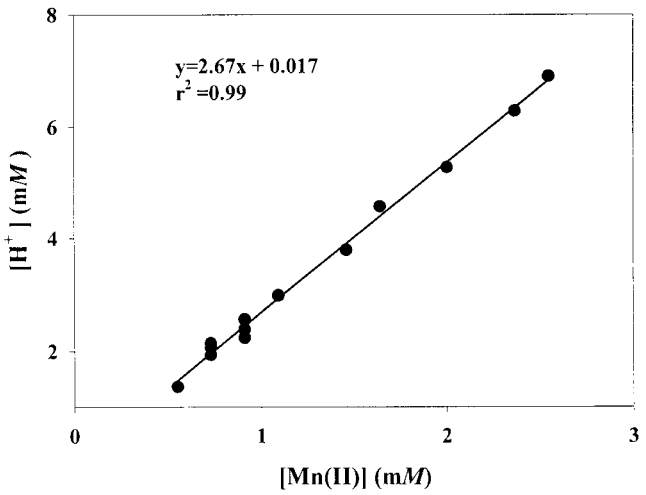

Fig. 2. Typical stoichiometry of H^+ consumed versus dissolved Mn(II) produced during birnessite reduction by catechol.

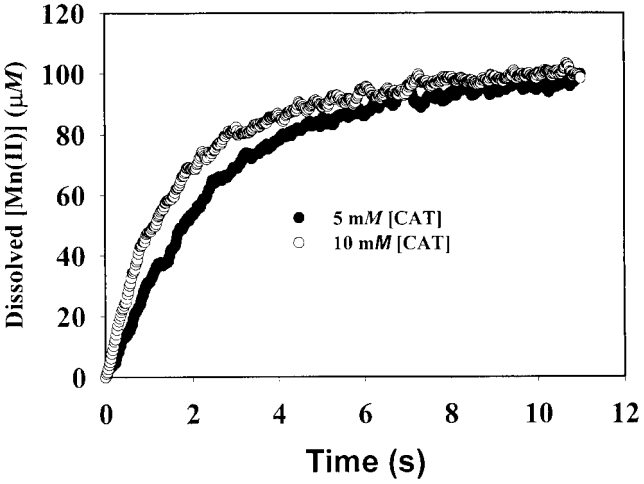

Fig. 3. Representative EPR-SF kinetics of reductive dissolution of birnessite by catechol at pH 4 as a function of [CAT] conducted at 23°C and 0.45 m^2 L^{-1} [SA].

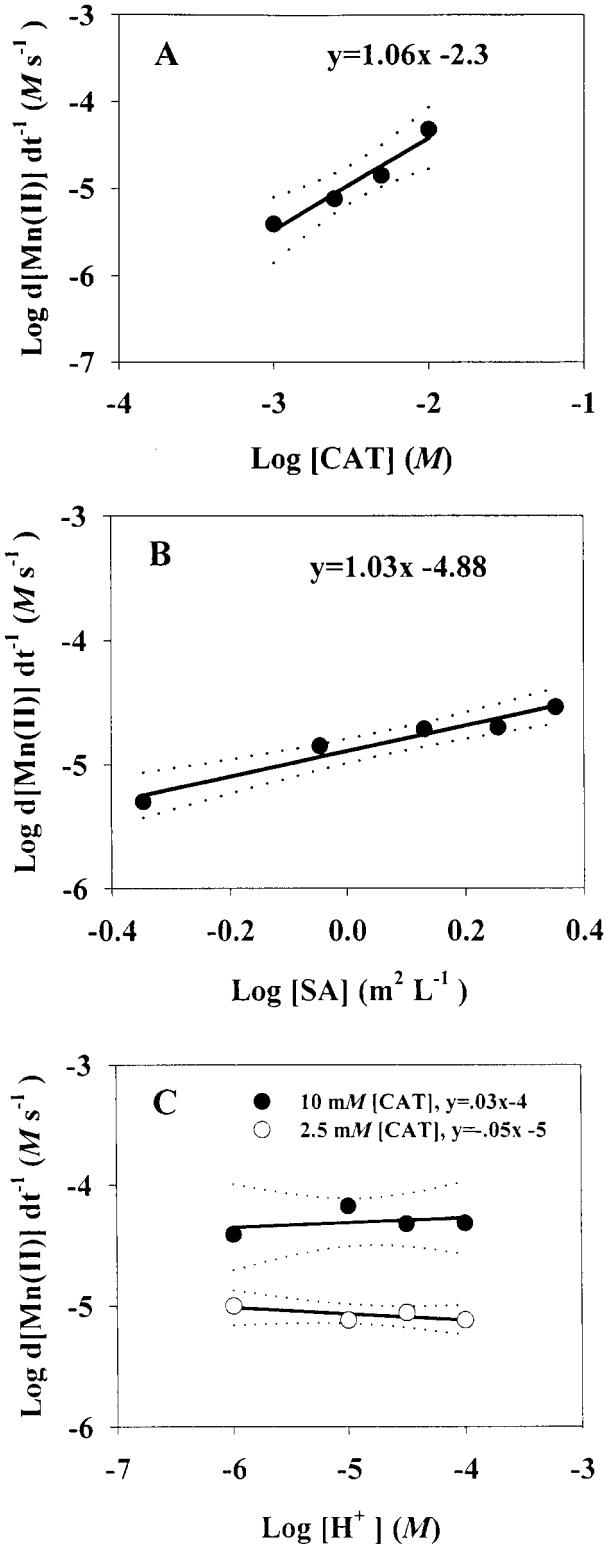

Fig. 4. Initial rate of dissolved Mn(II) release measured by the EPR-SF technique as a function of: (A) [CAT] at pH 4 and 0.90 m^2 L^{-1} [SA]; (B) [SA] at pH 4 and 5 (10^{-3} M [CAT]; and (C) [H$^+$] at 0.90 m^2 L^{-1} [SA]. The dotted lines represent the 95% confidence interval bands.

order rate constants k_{graph} and k_{calc} provides further support for the proposed rate equation.

It was anticipated on the basis of previous reports (Stone and Morgan, 1984a; Stone, 1987; Ukrainczyk and McBride, 1992; Xyla et al., 1992) that changes in pH might cause changes in the reductive dissolution rate of solid Mn-(III,IV) minerals by oxidizable organic ligands through (i) readsorption of Mn(II) at higher pH; (ii) proton-promoted dissolution at lower pH; (iii) a change in the thermodynamic driving force for the reaction; (iv) increased sorption of catechol on the pH-dependent charged surface of birnessite; and (v) speciation of catechol due to dissociation of the phenolic hydroxyl groups. The general lack of a pH effect may be explained by a combination of the low point of zero charge of the birnessite surface with the following pKs (Balistrieri and Murray, 1982):

$$>Mn^{IV}OH_2^+ \leftrightarrow >Mn^{IV}OH + H^+, \quad pK_{a1} = 2.3 \quad [5]$$

$$>Mn^{IV}OH \leftrightarrow >Mn^{IV}O^- + H^+, \quad pK_{a2} = 3.3 \quad [6]$$

and the low fraction of dissociated catechol (0.02%) calculated at the highest experimental pH (pH = 6) on the basis of the pK_{a1} = 9.7 and pK_{a2} = 13.7. The protonated form, the dominant catechol species under our experimental conditions, is generally considered less reactive toward oxidation than the deprotonated catecholate (McBride et al., 1988). These findings imply that the sorption affinity of birnessite for catechol to form a precursor surface complex should remain constant over the pH range employed.

Stability constants for sorption of organic ligands on metal (hydr)oxide surfaces are often proportional to stability constants for the metal-ligand complex in solution (Kummert and Stumm, 1980). Tris-$Mn^{IV}(cat)_3^{2-}$ and bis-$Mn^{III}(cat)_2^-$ complexes form in solution but are better described as $Mn^{II}(semi)_2(cat)^{2-}$ and $Mn^{II}(semi)(cat)^-$ because of internal metal-ligand redox reactions that convert catechol ligands to semiquinone ligands (Richert et al., 1988). The catechol to Mn(IV) ligand-to-metal-charge-transfer (LCMT) band was reported at 585 nm (Hartman et al., 1984) and the catechol to Mn(III) LCMT band between 550 and 750 nm (Magers et al., 1978). The chemical structure of catechol sorbed onto Al oxide and TiO_2 has been proposed to involve 1:1 (bidentate surface chelate complex) and 2:1 metal:ligand (binuclear) ratios (Kummert and Stumm, 1980; McBride and Wesselink, 1988; Rodriguez et al., 1996) and may resemble the surface complex between cate-

Table 2. Representative experimental conditions used to measure EPR-SF kinetic data.

[CAT]	pH (±0.05)	[SA]	k_{calc}
$\times 10^{-2}$ M		m^2 L^{-1}	$\times 10^{-3}$ L m^{-2} s^{-1}
1.00	4.0	0.91	5.3 ± 0.5†
0.50	4.0	0.91	3.2
0.25	4.0	0.91	3.4
0.1	4.0	0.91	4.3 ± 0.1
1.00	6.0	0.91	4.3 ± 0.3
0.50	6.0	0.91	5.6
0.25	6.0	0.91	4.4
0.1	6.0	0.91	4.5 ± 0.1
0.50	4.0	0.45	2.2 ± 0.2
0.50	4.0	1.42	2.8
0.50	4.0	1.78	2.2 ± 0.2
0.50	4.0	2.31	2.6

† Standard error of the mean.

chol and surface Mn in this study. Five-membered ring chelates are favored in coordination for steric and entropic reasons (Shriver et al., 1994). The "bite" (O-O) distance in the catecholate ligand of 2.77 Å may be compatible with surface Mn-Mn distances (assuming a 110 cleavage plane) in birnessite of 2.85 Å, suggesting that catechol may also form a binuclear precursor surface complex. The ability of catechol to bind two surface Mn metal centers may explain the observed rapid reductive dissolution rate. It should be pointed out that there is no spectroscopic evidence confirming the structure of the catechol-birnessite precursor surface complex, but past infrared spectroscopic studies have shown that it is difficult to identify (McBride, 1987). Currently, work in our laboratory is being conducted to observe the LCMT bands on the reacted birnessite using diffuse reflectance spectroscopy. Despite unfavorable sorption interactions between uncharged catechol (pK_{a1} = 9.7, pK_{a2} = 13.7) and the highly negatively charged birnessite surface (PZC ~2), in the pH range of most soils, catechol is extremely efficient at solubilizing Mn.

Catechol underwent oxidative transformation during reaction with an excess of birnessite (4.5 m^2 L^{-1}) at pH 4 to form *o*-quinone with concomitant release of Mn(II) (Fig. 5). Near complete mass balance indicates that the amount of catechol that reacted with birnessite can be accounted for by the production of the *o*-quinone monomer, the oxidation product expected to form via a two-electron transfer. First order rate plots (data not shown) were linear for catechol disappearance from solution ($r^2 > 0.99$) and yielded a pseudo-first order rate coefficient k_c for catechol disappearance of 0.70 (±0.18) min^{-1}. This compares well with the kinetics of *o*-quinone and Mn(II) appearance (k_o = 0.61 min^{-1} and k_m = 0.55 min^{-1}) indicating that electron transfer was rapid. These results strongly suggest that catechol sorption to form a precursor surface complex was rate-limiting and product sorption was not affecting the reaction rate.

The suggestion that precursor surface complex formation was rate-limiting is supported by the activation

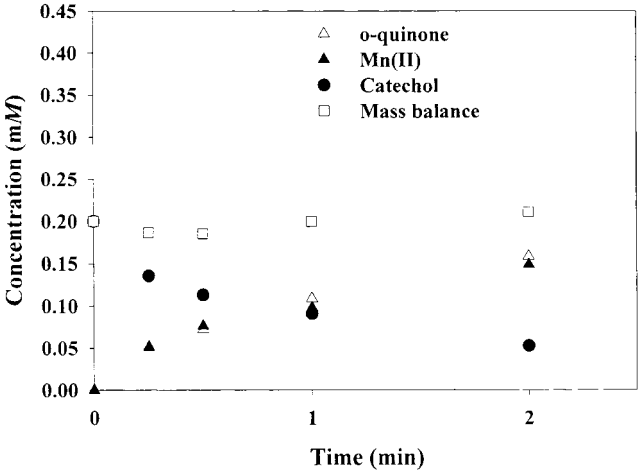

Fig. 5. Kinetics of catechol oxidation to *o*-quinone by birnessite and dissolved Mn(II) release at 23°C. Experimental conditions were: [CAT] = 0.2 m*M*, [SA] = 4.5 m^2 L^{-1}([Mn_T] = 1 m*M*), pH 4, I = 0.01 *M* NaCl.

Table 3. Activation parameters describing the reductive dissolution of birnessite by catechol.

Parameter	Birnessite/catechol system
E_a†, kJ mol^{-1}	58.7 ± 6.6‡
ln A	21.1 ± 2.7
$\Delta H^{\ddagger}$, kJ mol^{-1}	56.2 ± 6.6
$\Delta S^{\ddagger}$, J mol^{-1} K^{-1}	−77.9 ± 22.4
$\Delta G^{\ddagger}$, kJ mol^{-1}	32.9 ± 13.3

† E_a (energy of activation), ln A (pre-exponential factor), $\Delta H^{\ddagger}$ (enthalpy of activation), $\Delta S^{\ddagger}$ (entrophy of activation), and $\Delta G^{\ddagger}$ (free energy of activation) were derived from Arrhenius and Eyring plots.
‡ Standard error of the mean.

parameters (Table 3) derived by Arrhenius and Eyring plots (Fig. 6). The activation energy (E_a) of 59 (±7) kJ mol^{-1} suggests that the reaction was surface-chemical controlled (Lasaga, 1981; Sparks, 1989, 1995) and agrees with previous reductive dissolution studies (Stone and Morgan, 1984a). Other investigators have proposed that electron transfer was the rate-limiting step and have treated precursor complex formation as a preequilibrium step (Stone and Morgan, 1984a; Stone and Morgan, 1987). The high positive value for $\Delta H^{\ddagger}$ (56 ± 7 kJ mol^{-1}) and negative value for $\Delta S^{\ddagger}$ (−78 ± 22 J mol^{-1} K^{-1}) suggests the possibility of a bimolecular step, which is

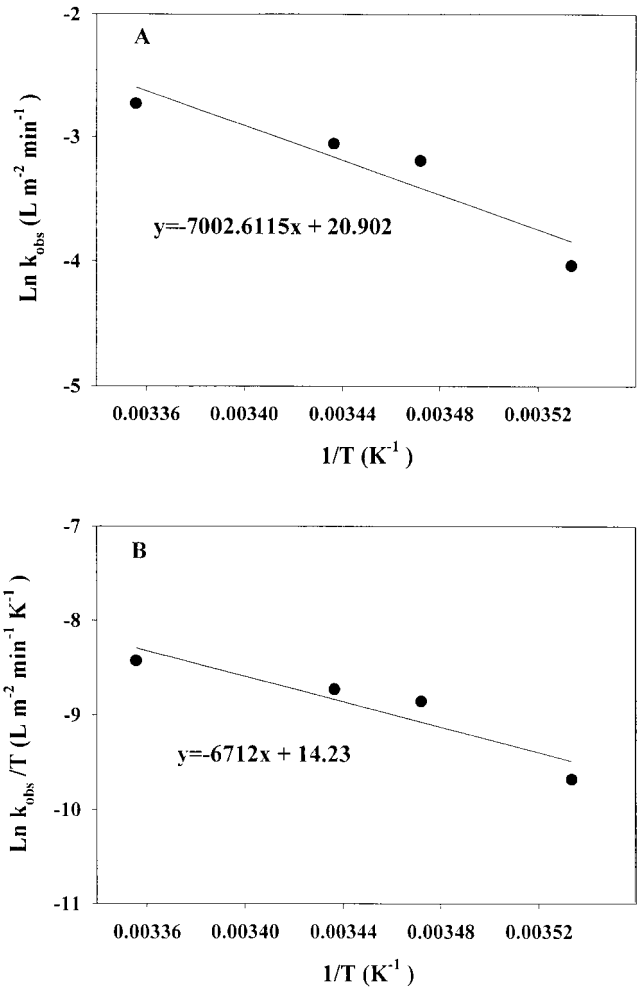

Fig. 6. Activation parameters derived from (A) Arrhenius and (B) Eyring plots describing the reductive dissolution of birnessite by catechol.

common to second-order reactions (Espenson, 1995). The observed second-order rate constant measured from EPR-SF studies indicated a more rapid reaction than would be expected from the high activation energy. However, the high activation energy can be compensated for by the large negative $\Delta S^{\ddagger}$ value to yield a fast reaction (Espenson, 1995).

Proposed Reaction Mechanism

These results provide further support for the general reaction mechanism initially proposed by Stone and Morgan (1984a) for reductive dissolution of Mn oxides. Formally, the reaction scheme includes the following steps.

Precursor Surface Complex Formation

$$C_6H_4(OH)_2\ (aq) + >\delta\text{-}MnO_2\ (s) \underset{k_{-1}}{\overset{k_1}{\leftrightarrow}} >\delta\text{-}MnO_2 - C_6H_4(OH)_2\ (s) \qquad [7]$$

Electron Transfer within the Surface Complex

$$>\delta\text{-}MnO_2 - C_6H_4(OH)_2(s) \underset{k_{-2}}{\overset{k_2}{\leftrightarrow}} >Mn(II) - C_6H_4O_2(s) + 2OH^- \qquad [8]$$

Product Release

$$>Mn(II) - C_6H_4O_2\ (s) \underset{k_{-3}}{\overset{k_3}{\leftrightarrow}} Mn(II)(aq) + >C_6H_4O_2(s) \qquad [9]$$

$$>C_6H_4O_2(s) \underset{k_{-4}}{\overset{k_4}{\leftrightarrow}} C_6H_4O_2(aq) \qquad [10]$$

The activation parameters indicate that the reaction is surface chemical controlled (Table 3). The simultaneous release of Mn(II) and *o*-quinone (Fig. 5) indicated that $k_3 \approx k_4$ and back reactions are negligible ($k_{-3} \approx k_{-4} = 0$). The mass balance results, the pseudo-first order decay in catechol solution concentration, and the immediate product release imply that $k_2 > k_1$ and that precursor surface complex formation as shown in Eq. [7] was rate-limiting. The pH independent rate equation provided further support of Eq. [7] as the rate-limiting step. The value for $\Delta S^{\ddagger}$ (-78 J mol^{-1} K^{-1}) supports an associative ligand substitution mechanism in which the E_a is determined primarily by the energy required for bond formation of the entering group (catechol) to the Mn(IV) surface sites (Atwood, 1997). The empirical rate equation was internally consistent with an associative mechanism based on the observed first order dependence on [CAT] (see Eq. [4] and Shriver et al., 1994). After precursor surface complex formation, two electrons can be immediately transferred along the bonding axis as an inner sphere process from the filled catechol *p* orbitals of σ symmetry to the empty e_g (σ^*) orbitals of the Mn(IV) metal centers. The Mn-catechol bond could be formed with electron transfer before the Mn-O bond cleaves, which is characteristic of associative mechanisms (Shriver et al., 1994). Frontier-molecular-orbital-theory (FMOT) predicts a large driving force for electron transfer because of the vacant σ^* orbitals in Mn(IV) (Luther, 1990; Luther et al., 1998). On the basis of our data, no distinction can be made between two one-electron transfers or a single concerted two-electron transfer nor whether the electrons are transferred as a hydrogen atom (H•) or hydride (H-) ion. The rapid formation of *o*-quinone, however, would suggest a concerted two-electron transfer step. Perez-Benito et al. (1996) reported a possible direct two-electron transfer from oxalate to Mn(IV) in soluble MnO_2. Further experiments are being conducted to substantiate the proposed reaction mechanism.

CONCLUSIONS

In this study, mechanisms of reductive dissolution of birnessite by catechol were studied by EPR-SF and stirred-batch techniques. The reaction was rapid and independent of pH under the experimental conditions of this study (pH 4 to 6). Kinetic and thermodynamic results indicate direct attack of aqueous catechol on birnessite by an associative ligand substitution mechanism to form a precursor surface complex with surface Mn oxide sites. Formation of the precursor surface complex is likely the rate-limiting step as detrermined on the basis of the experimentally determined activation energy of 59 ($\pm$7) kJ mol^{-1} and the comparable rates of catechol disappearance and product formation. Our results indicate that catechol could serve as an alternative soil extractant for easily reducible Mn between pH 4 to 6 as detrermined on the basis of the rapid reductive dissolution kinetics. Excessive levels of catechol in natural soil environments could possibly lead to Mn toxicity in susceptible plants.

ACKNOWLEDGMENTS

We thank Dr. A.T. Stone for providing publications, Drs. G.W. Luther III and C.G. Riordan for fruitful discussions, and an anonymous reviewer for constructive comments. C.J. Matocha appreciates the hospitality extended by the staff at the EMSL while conducting the EPR-SF studies and the support of a DuPont Graduate Research Fellowship. The EMSL is funded by the Office of Biological and Environmental Research in the U.S. Department of Energy and operated by Battelle as part of the Pacific Northwest National Laboratory under Contract DE-AC06-76RLO.

REFERENCES

Alexander, M. 1977. Introduction to soil microbiology. John Wiley & Sons, New York.

Amonette, J.E., F.A. Khan, A.D. Scott, H. Gan, and J.W. Stucki. 1994. Quantitative oxidation-state analysis of soils. p. 83–113. *In* J.E. Amonette and L.W. Zelazny (ed.) Quantitative methods in soil mineralogy. SSSA Misc. Publ. SSSA, Madison, WI.

Atwood, J.D. 1997. Inorganic and organometallic reaction mechanisms. VCH Publishers, New York.

Balistrieri, L.S., and J.W. Murray. 1982. The surface chemistry of

δ-MnO_2 in major ion seawater. Geochim. Cosmochim. Acta. 46: 1041–1052.
Bartlett, R.J. 1981. Nonmicrobial nitrite-to-nitrate transformation in soils. Soil Sci. Soc. Am. J. 45:1054–1058.
Bartlett, R.J., and B.R. James. 1993. Redox chemistry of soils. Adv. Agron. 50:151–208.
Bricker, O. 1965. Some stability relations in the system Mn-O_2-H_2O at 25° and one atmosphere total pressure. Am. Mineral. 50:1296–1354.
Brunauer, C.A., P.H. Emmett, and E. Teller. 1938. Adsorption of gases in multi-molecular layers. J. Am. Chem. Soc. 60:309–319.
Carpenter, R. 1983. Quantitative electron spin resonance (ESR) determinations of forms and total amounts of Mn in aqueous environmental samples. Geochim. Cosmochim. Acta. 47:875–885.
Cheney, M.A., G. Sposito, A.E. McGrath, and R.S. Criddle. 1996. Abiotic degradation of 2,4-D (dichlorophenoxyacetic acid) on synthetic birnessite: A calorespirometric method. Colloids and Surfaces 107:131–140.
Davies, G. 1969. Some aspects of the chemistry of manganese(III) in aqueous solution. Coor. Chem. Rev. 4:199–224.
Dawson, C.R., and J.M. Nelson. 1938. The influence of catechol on the stability of o-benzoquinone in aqueous solutions. J. Am. Chem. Soc. 60:245–249.
Dec, J., and J.M. Bollag. 1994. Dehalogenation of chlorinated phenols during oxidative coupling. Environ. Sci. Technol. 28:484–490.
Diebler, H., and N. Sutin. 1964. The kinetics of some oxidation-reduction reactions involving manganese(III). J. Phys. Chem. 68: 174–180.
Drits, V.A., E. Silvester, A.I. Gorshkov, and A. Manceau. 1997. Structure of synthetic monoclinic Na-rich birnessite and hexagonal birnessite: I. Results from x-ray diffaction and selected-area electron diffraction. Am. Mineral. 82:946–961.
Espenson, J.H. 1995. Chemical kinetics and reaction mechanisms. 2nd ed. McGraw-Hill, New York.
Fendorf, S.E., D.L. Sparks, J.A. Franz, and D.M. Camaioni. 1993. Electron paramagnetic resonance stopped-flow kinetic study of manganese(II) sorption-desorption on birnessite. Soil Sci. Soc. Am. J. 57:57–62.
Godtfredsen, K.L., and A.T. Stone. 1994. Solubilization of manganese dioxide-bound copper by naturally occurring organic compounds. Environ. Sci. Technol. 28:1450–1458.
Gordon, G., and H. Taube. 1962. Oxygen tracer experiments on the oxidation of aqueous uranium(IV) with oxygen-containing oxidizing agents. Inorg. Chem. 1:69–75.
Hartman, J.R., B.M. Foxman, and S.R. Cooper. 1984. Higher valent manganese chemistry. Synthetic, structural, and solution studies on $[Mn(catecholate)_3]^{n-}$ (n = 2,3) complexes. Inorg. Chem. 23: 1381–1387.
Hem, J.D. 1978. Redox processes at surfaces of manganese oxide and their effects on aqueous metal ions. Chem. Geol. 21:199–218.
Hersman, L., T. Lloyd, and G. Sposito. 1995. Siderophore-promoted dissolution of hematite. Geochim. Cosmochim. Acta. 59:3327–3330.
Hubbell, W.L., W. Froncisz, and J.S. Hyde. 1987. Continuous and stopped flow EPR spectrometer based on a loop gap resonator. Rev. Sci. Instrum. 58:1879–1886.
Klimes, N., G. Lassmann, and B. Ebert. 1980. Time-resolved EPR spectroscopy. Stopped-flow EPR apparatus for biological application. J. Magn. Reson. 37:53–59.
Kostka, J.E., G.W. Luther III, and K.H. Nealson. 1995. Chemical and biological reduction of Mn(III)-pyrophosphate complexes: Potential importance of dissolved Mn(III) as an environmental oxidant. Geochim. Cosmochim. Acta 59:885–894.
Kummert, R., and W. Stumm. 1980. The surface complexation of organic acids on hydrous g-Al_2O_3. J. Colloid Interface Sci. 75: 373–385.
Laha, S., and R.G. Luthy. 1990. Oxidation of aniline and other primary aromatic amines by manganese dioxide. Environ. Sci. Technol. 24:363–373.
Larsen, F., and D. Postma. 1997. Nickel mobilization in a groundwater well field: Release by pyrite oxidation and desorption from manganese oxides. Environ. Sci. Technol. 31:2589–2595.
Lasaga, A.C. 1981. Rate laws of chemical reactions. p. 1–68. *In* A.C. Lasaga and R.J. Kirkpatrick (ed.) Kinetics of geochemical processes. Reviews in mineralogy, Vol. 8. Mineralogical Society of America, Washington, DC.
Lindberg, R.D., and D.D. Runnells. 1984. Ground water redox reactions: An analysis of equilibrium state applied to E_h measurements and geochemical modeling. Science 225:925–927.
Luca, V., and C.M. Cardile. 1989. Cation migration in smectite minerals: Electron spin resonance of exchanged Fe^{3+} probes. Clays Clay Miner. 37:325–332.
Luther, G.W. III. 1990. Frontier molecular orbital theory in geochemical processes. p. 173–198. *In* W. Stumm (ed.) Aquatic chemical kinetics: Reaction rates of processes in natural water. Wiley-Interscience, New York.
Luther, G.W. III, D.T. Ruppel, and C. Burkhard. 1998. Reactivity of dissolved Mn(III) complexes and Mn(IV) species with reductants: Mn redox chemistry without a dissolution step? p. 265–280. *In* D.L. Sparks and T.J. Grundl (ed.) Mineral-water interfacial reactions: Kinetics and mechanisms. ACS Symposium Ser. No. 715, Washington.
Luther, G.W. III, B. Sundby, B.L. Lewis, P.J. Brendel, and N. Silverberg. 1997. Interactions of manganese with the nitrogen cycle: alternative pathways to dinitrogen. Geochim. Cosmochim. Acta 61:4043–4052.
Magers, K.D., C.G. Smith, and D.T. Sawyer. 1978. Polarographic and spectroscopic studies of the manganese(II), -(III), and –(IV) complexes formed by polyhydroxy ligands. Inorg. Chem. 17: 515–523.
Manceau, A., A.I. Gorshkov, and V.A. Drits. 1992. Structural chemistry of Mn, Fe, Co, and Ni in manganese hydrous oxides: Part I. Information from XANES spectroscopy. Am. Miner. 77:1133–1143.
Mason, H.S. 1949. The chemistry of melanin. VI. Mechanism of the oxidation of catechol by tyrosinase. J. Biol. Chem. 181:803–812.
McBride, M.B. 1987. Adsorption and oxidation of phenolic compounds by iron and manganese oxides. Soil Sci. Soc. Am. J. 51:1466–1472.
McBride, M.B., F.J. Sikora, and L.G. Wesselink. 1988. Complexation and catalyzed oxidative polymerization of catechol by aluminum in acidic solution. Soil Sci. Soc. Am. J. 52:985–993.
McBride, M.B. 1989a. Oxidation of dihydroxybenzenes in aerated aqueous suspensions of birnessite. Clays Clay Miner. 37:341–347.
McBride, M.B. 1989b. Oxidation of 1,2- and 1,4-dihydroxybenzene by birnessite in acid aqueous suspension. Clays Clay Miner. 37:470–486.
McBride, M.B., and L.G. Wesselink. 1988. Chemisorption of catechol on gibbsite, boehmite, and noncrystalline alumina surfaces. Environ. Sci. Technol. 22:703–708.
McKenzie, R.M. 1971. The synthesis of birnessite, cryptomelane, and some other oxides and hydroxides of manganese. Mineral. Mag. 38:493–502.
McKenzie, R.M. 1989. Manganese oxides and hydroxides. p. 439–465. *In* J.B. Dixon and S.B. Weed (ed.) Minerals in soil environments. 2nd ed. SSSA Book Series 1. SSSA, Madison, WI.
Mentasti, E., E. Pelizzetti, E. Pramauro, and G. Giraudi. 1975. Redox reaction of 1,2-dihydroxybenzene in aqueous perchlorate media. Kinetics and mechanism. Inorg. Chim. Acta 12:61–65.
Moore, J.N., J.R. Walker, and T.H. Hayes. 1990. Reaction scheme for the oxidation of As(III) to As(V) by birnessite. Clays Clay Miner. 38:549–555.
Murray, J.W. 1974. The surface chemistry of hydrous manganese dioxide. J. Colloid Inter. Sci. 46:357–371.
Murray, J.W., L.S. Balistrieri, and B. Paul. 1984. The oxidation state of manganese in marine sediments and ferromanganese nodules. Geochim. Cosmochim. Acta 48:1237–1247.
Naidja, A., P.M. Huang, and J.M. Bollag. 1998. Comparison of reaction products from the transformation of catechol catalyzed by birnessite or tyrosinase. Soil Sci. Soc. Am. J. 62:188–195.
Perez-Benito, J.F., C. Arias, and E. Amat. 1996. A kinetic study of the reduction of colloidal manganese dioxide by oxalic acid. J. Colloid Interface Sci. 177:288–297.
Pizzigallo, M.D.R., P. Ruggiero, C. Crecchio, and R. Mininni. 1995. Manganese and iron oxides as reactants for oxidation of chlorophenols. Soil Sci. Soc. Am. J. 59:444–452.
Richert, S.A., P.K.S. Tsang, and D.T. Sawyer. 1988. Ligand-centered oxidation of manganese(II) complexes. Inorg. Chem. 27:1814–1818.
Rodríguez, R., M.A. Blesa, and A.E. Regazzoni. 1996. Surface complexation at the TiO_2 (anatase)/aqueous solution interface: Chemisorption of catechol. J. Colloid Interface Sci. 177:122–131.

Schulze, D.G., T. McCay-Buis, S.R. Sutton, and D.M. Huber. 1995a. Manganese oxidation states in *Gaeumannomyces*-infested wheat rhizospheres probed by micro-XANES spectroscopy. Phytopathology 85:990–994.

Schulze, D.G., S.R. Sutton, and S. Bajt. 1995b. Determining manganese oxidation state in soils using x-ray absorption near-edge structure (XANES) spectroscopy. Soil Sci. Soc. Am. J. 59:1540–1548.

Shindo, H., and P.M. Huang. 1982. Role of Mn(IV) oxide in abiotic formation of humic substances in the environment. Nature 298:363–365.

Shindo, H., and P.M. Huang. 1984. Catalytic effects of manganese(IV), iron(III), aluminum, and silicon oxides on the formation of phenolic polymers. Soil Sci. Soc. Am. J. 48:927–934.

Shriver, D.F., P. Atkins, and C.H. Langford. 1994. Inorganic chemistry. 2nd ed. W.H. Freeman and Co., New York.

Silvester, E., A. Manceau, and V.A. Drits. 1997. Structure of synthetic monoclinic Na-rich birnessite and hexagonal birnessite: II. Results from chemical studies and EXAFS spectroscopy. Am. Mineral. 82:962–978.

Sparks, D.L. 1989. Kinetics of soil chemical processes. Academic Press, New York.

Sparks, D.L. 1995. Environmental soil chemistry. Academic Press, San Diego, CA.

Stach, J., R. Kirmse, W. Dietzsch, G. Lassman, V.K. Belyaeva, and I.N. Marov. 1985. Ligand exchange reactions between copper(II)- and nickel(II)-chelates of different sulfur-and selenium-containing ligands. VI [1]. Kinetics of ligand exchange reactions studied by stopped-flow ESR. Inorg. Chim. Acta 96:55–59.

Steelink, C. 1964. Free radical studies of lignin, lignin degradation products and soil humic acid. Geochim. Cosmochim. Acta. 28: 1615–1622.

Stone, A.T. 1987. Reductive dissolution of manganese (III/IV) oxides by substituted phenols. Environ. Sci. Technol. 21:979–988.

Stone, A.T., K.L. Godtfredsen, and B. Deng. 1994. Sources and reactivity of reductants encountered in aquatic environments. p. 337–374. *In* G. Bidoglio and W. Stumm (ed.) Chemistry of aquatic systems: Local and global perspectives. ECSC, The Netherlands.

Stone, A.T., and J.J. Morgan. 1984a. Reduction and dissolution of manganese (III) and manganese (IV) oxides by organics. 1. Reaction with hydroquinone. Environ. Sci. Technol. 18:450–456.

Stone, A.T., and J.J. Morgan. 1984b. Reduction and dissolution of manganese (III) and manganese (IV) oxides by organics. 2. Survey of the reactivity of organics. Environ. Sci. Technol. 18:617–624.

Stone, A.T., and J.J. Morgan. 1987. Reductive dissolution of metal oxides. p. 221–254. *In* W. Stumm (ed.) Aquatic surface chemistry: Chemical processes at the particle-water interface. Wiley, New York.

Ukrainczyk, L., and M.B. McBride. 1992. Oxidation of phenol in acidic aqueous suspensions of manganese oxides. Clays Clay Minerals 40:157–166.

Ukrainczyk, L., and M.B. McBride. 1993a. The oxidative dechlorination reaction of 2,4,6-trichlorophenol in dilute aqueous suspensions of manganese oxides. Environ. Toxicol. Chem. 12:2005–2014.

Ukrainczyk, L., and M.B. McBride. 1993b. Oxidation and dechlorination chlorophenols in dilute aqueous suspensions of manganese oxides: Reaction products. Environ. Toxicol. Chem. 12:2015–2022.

Wang, M.C., and P.M. Huang. 1987. Polycondensation of pyrogallol and glycine and the associated reactions as catalyzed by birnessite. Sci. Total Environ. 62:435–442.

Wang, M.C., and P.M. Huang. 1992. Significance of Mn(IV) oxide in the abiotic ring cleavage of pyrogallol in natural environments. Sci. Total Environ. 113:147–157.

Xyla, A.G., B. Sulzberger, G.W. Luther III, J.G. Hering, P. van Cappellen, and W. Stumm. 1992. Reductive dissolution of manganese (III,IV) (hydr)oxides by oxalate: The effect of pH and light. Langmuir 8:95–103.